Electrical Heating And Piezoresistive Characteristics Of Hierarchical Cuo-Carbon Fiber Laminates

Ravi Kumar Cheedarala[1,2] *, K A Emmanuel[1] and NVVS Prasad[1]

[1] *Dr. K A Emmanuel, Associate Professor, Sir C R Reddy Autonomous College, Adikavi Nanaiah University, ELURU, India.*
[1] *Dr. N V V S Prasad, Associate Professor, Sir C R Reddy Autonomous College, Adikavi Nanaiah University, ELURU, India.*
[2] *Dr. Ravi Kumar Cheedarala, Research Professor, School of Mechanical Engineering, University of Ulsan, 93 Daehak-ro, Nam-gu, Ulsan, South Korea.*

Abstract: *The electric heating and piezoresistive characteristics of CuO–woven carbon fiber (CuO–WCF) composite laminates were experimentally evaluated. Hybrid CuO–WCF composites were fabricated via a two-step seed-mediated hydrothermal method. The interlaminar interface between two plies of hybrid CuO–WCF/vinyl ester composite laminae was influenced by interlocked fiber–fiber cross-linking structures with CuO NRs and acted as electric heating and resistance elements. The contribution of CuO NRs (10–110 mM) to the interlaminar interface was determined by measuring the temperature profile, in order to investigate the electrical resistive heating behavior. At higher concentration of CuO NRs growth in the interlaminar region applied by 3 A, the average temperature reached to 83.55 °C at the interface area 50×50 mm^2 and the heating efficiency was 0.133 W/°C owing to radiation and convection given by 10.5 W (3 A, 3.5 V). To investigate the piezoresistive response, the through-thickness gauge factor was observed at 0.312 during Joule heating applied by 2 A, compared with 0.639 at an ambient air temperature for CuO 110 mM concentration. The morphology and crystallinity of CuO NRs were investigated using scanning electron microscopy and X-ray diffraction analyses, respectively. The temperature dependence of hybrid CuO–WCF composite laminates' storage moduli were analyzed using a dynamic mechanical analyzer. These characterizations showed that the interlaminar interface, combined with the high specific surface area of CuO NRs, provided the electron traps for electrical conduction around multiple WCF junctions and adjacent cross-linked laminae.*

Keywords: *Carbon fiber, Functional composites, Oxides, Thermal properties, Interface*

I. INTRODUCTION

In recent years, multifunctional materials and composite structures have drawn considerable interest for use in both structural and non-structural applications. Most of the mechanical development in structural functionalized materials aims to increase the specific strength, specific stiffness, and fracture toughness of a given material. In contrast, non-structural functionalized materials often require diverse properties such as electrical or thermal conductivity, sensing capabilities, energy harvesting/storage abilities, self-healing capabilities, electromagnetic interference shielding, recyclability, and biodegradability [1,2].

Polymer–matrix composites with carbon fibers boast both structural and non-structural functions and are used in various commodity and engineering applications requiring high specific strength, stiffness, light weight, and high thermal and electrical conductivities [3–5]. However, attaining desirable non-structural functions while maintaining the desired structural properties depends strongly on the interfacial interactions within the fiber–matrix interface, which govern the overall performance of a composite material [6]. Several researchers have reported various strategies to obtain desired non-structural functions in composite materials.

Whiskerization, a representative technique used to tailor interfacial interactions, results in a graded interface that reduces stress between the fiber and matrix phases. In composites, whiskerization is normally deposited in an array of whiskers onto the fiber and yields improvement of cohesion between fiber and matrix. Hence, the interphase properties are enhanced due to interlocking the matrix–fiber interface. CuO-grafted on the surface of fiber, one of the whiskerization tailored on the fiber, has been reported to get higher mechanical properties of composites because of the crosslinked network acting as the enhanced load-bearing capacity due to the higher specific surface area of CuO [7,8]. CuO whiskers are promising in this regard due to their typical p-type semiconductor structure with a narrow band gap of ~1.2 eV. CuO whiskers also exhibit non-structural functions that have been shown useful in various applications including gas sensors, lithium-copper oxide electrochemical cells, magnetic storage media, and solar energy transformers [9–12].

II. Experimental

2.1. Materials

T-300 grade plain WCFs were obtained from Toray Industries Inc. (Japan). To prepare hybrid CuO–WCFs, analytical grade chemicals for seed and growth solutions were provided by Sigma–Aldrich (U.S.A.). These included copper acetate monohydrate ($Cu(CH_3COO)_2 \cdot H_2O$), sodium hydroxide (NaOH), copper nitrate trihydrate ($Cu(NO_3)_2 \cdot 3H_2O$), and hexamethylenetetramine ($C_6H_{12}N_4$, HMTA). Ethanol was obtained from J.T. Baker, Philipsburg, NJ, U.S.A. and was used as a solvent for copper acetate monohydrate to obtain a stable colloidal suspension of CuO seeds on WCFs.

2.2. Preparation of hybrid CuO–WCF composite laminates

Fig. 1 shows a two-step seed-mediated hydrothermal process used to synthesize the hybrid CuO–WCF. This method is relatively simple and allows low-temperature processing of nano-structured components. The seed solution was prepared from a solution of $Cu(CH_3COO)_2 \cdot H_2O$ and NaOH. The CuO seed layer on WCF was prepared by soaking the WCF in the seed solution for 10 min and then annealing the seed-coated WCF in a hot furnace at 150 °C for 10 min. Reaction (4) shows that CuO was grown from OH^- and Cu^{2+}[23]. Further details of these synthetic routes can be found in the literature [24]. Hybrid CuO–WCF/vinyl ester composite laminates were formed using the VARTM process and infiltrated with vinyl ester resin, initiator, and an accelerating agent at a ratio of 100:1:1 by weight. The contributions of CuO NRs in the interlaminar interface were investigated by studying the surface morphology, crystallinity, dynamic mechanical properties, electric heating behavior, and piezoresistive response of the composite material under flexural tests during thermal heating and at ambient air temperature.

2.3. Evaluation of the electrical and piezoresistive properties of the interlaminar interface

To determine the electrical resistive heating behavior of the composites, infrared thermographic analyses were performed using an infrared camera (H2640, Joowon Industrial Co., Ltd., Korea). The temperature gap was controlled by thermocouples placed on the sample. Two current (outer) and two voltage (inner) electrodes were attached to each upper and lower lamina, respectively, so current flow orthogonal to the laminae generated resistive heating at the interlaminar interface (between two laminae). The sample size was 80×80 mm^2 and the distance between the voltage electrodes was 50 mm. The specific experimental configuration is shown for an equivalent circuit in Fig. 2A.

The piezoresistivity of the hybrid CuO–WCF composite laminates was analyzed *in situ* using a digital multimeter (81/2-digit Model 2002, Keithley, U.S.A.) during a three-point bending test with the universal material testing system (Instron 5982, USA), as shown in Fig. 2B. Upon the flexure, the interlaminar interface of the prepared composite laminates was subjected to the two-dimensional array of fiber junctions with CuO NRs of two adjacent laminae with negligible microstructural damages due to reversible elastic deformation.
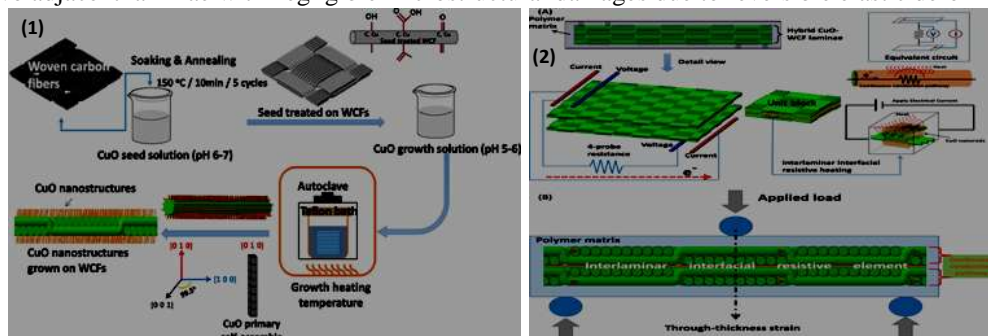
Fig. 1. Synthesis of hybrid CuO–WCF using a two-step seed-mediated hydrothermal method. **Fig. 2.** Schematic showing the (A) electrical resistive heating behavior and (B) piezoresistive response of the interlaminar interface in hybrid CuO–WCF composite laminates.

The degree of contact for CuO grafted on a WCF lamina increases around the polymer resin along the longitudinal (fiber) direction due to the multi-junctions of accumulated CuO NRs in the interface region between the fiber and matrix during flexural loading pressure. Flexural strain on the hybrid CuO–WCF composite laminates was applied at a strain rate of 1.6% min^{-1} under cyclic flexural loading for five cycles. The initial interlaminar resistance (R_0) was collected for 30 s to guarantee stability of the readings prior to cyclic loading. The piezoresistive effect of the hybrid CuO–WCF composite laminates was quantified by the gauge factor (GF, *k*), as shown in below [25]

$$k = \Box R/R0 \Box$$

where *k* is the calculated resistance change ($\Delta R/R0$) in response to an applied strain (ε) at a given temperature. In this study, the gauge factor indicates through-thickness gauge factor on account of fractional

changes in through-thickness resistance accompanied by through-thickness strain. The through-thickness resistance is equal to the interlaminar resistance between the two plied sheets. Both resistance and strain were measured during the maximum temperature plateau of the interlaminar resistive heating zone. This is discussed further in Section 3.4.

To eliminate electrode contact resistance, a four-point probe method was used, consisting of two outer current probes and two inner voltage probes (all made of silver). Four-point probe method yields the volume resistance, whereas the two-probe method yields the contact resistance. Hence, to investigate the piezoresistivity, which is the change of the volume electrical resistivity with strain, four-probe method was necessarily configured to the sample [26,27]. Each current and voltage electrode contact was placed in silver wire sealed with conducting silver paste on the upper and lower sheet. These electrodes were attached to an electrical power supply and the temperature distribution through each sample was monitored. The overall experimental configuration has been modified with the previous work [28].

2.4. Characterization

The morphology of CuO NRs grafted on the WCF surface at various CuO molar concentrations (10–110 mM) was studied by SEM. X-ray diffractograms (Bruker, U.S.A.) of the CuO NRs grafted on the WCF surface were analyzed with crystal monochromated Cu Kα radiation ($\lambda = 1.5418$ Å) from 30° to 80° (2θ) at a 1°/min scanning speed and an operating voltage of 40 kV and current of 200 mA. The dynamic mechanical thermal properties of the composite samples containing CuO NRs were analyzed using rectangular coupons measuring $12.0 \times 60.0 \times 0.6$ mm and a DMA (Q800 tester, TA Instruments, Inc., U.S.A.) in flexural mode from 50 to 200 °C at a heating rate of 1 °C/min and a frequency of 1 Hz with dual cantilever clamps in accordance with ASTM D5418-07.

III. Results and discussion

3.1. Morphology and crystallographic analyses

The morphologies of CuO NRs were controlled via the concentrations of copper nitrate trihydrate and HMTA precursor chemicals between 10 and 110 mM using a two-step seed-mediated hydrothermal method as shown in Fig. 3. CuO formations were similar to nanorods grown preferentially along the [0 1 0] direction. Higher OH^- concentrations encouraged growth along the [0 1 0] direction by increasing the $L_{[010]}/L_{[100]}$ and $L_{[100]}/L_{[001]}$ aspect ratios that govern self-aligned assembly into various microstructures [22]. Thus, the growth mechanism of CuO is influenced by NH_3 molecules that passivate the surface. Aggregates then form coordinate bonds with Cu^{2+} ions [20]. In a sealed autoclave at the proper temperature, these ions then react with Cu^{2+} ions in the growth solution. In this way, CuO self-aligns predominantly along the [0 1 0] direction while prohibiting attachment at the [1 0 0] and [0 1 0] directional planes because of the buffer conditions inside of the Teflon-lined bath. Water is the only by-product of the final chemical reaction. Thus, Cu^{2+} ions form strong ionic bonds with the carboxylic functional group of WCF.
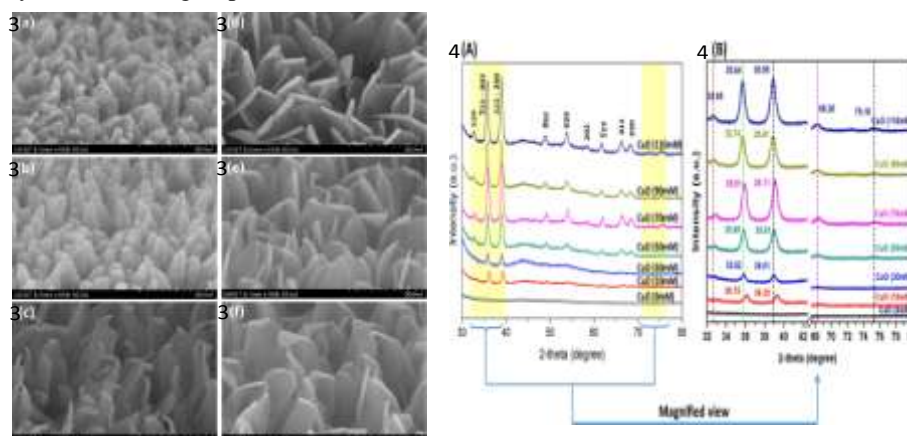
Fig. 3. Morphologies of CuO on WCF. CuO was grown at 120 °C for 12 h. The initial concentration of CuO in the growth solution was (a) 10 mM, (b) 30 mM, (c) 50 mM, (d) 70 mM, (e) 90 mM, and (f) 110 mM. The scale bar shown in the SEM micrographs corresponds to 300 nm. **Fig. 4.** X-ray diffractograms of hybrid CuO–WCFs at (A) various CuO growth concentrations and (B) under higher magnification.

Fig. 4A shows the X-ray diffractograms of hybrid CuO–WCF and pristine WCF (CuO 0 mM). All of the samples had the same phase structure, which was indexed to the monoclinic CuO crystal phase, with lattice parameters $a = 4.68$ Å, $b = 3.43$ Å, $c = 5.13$ Å and $\beta = 99.5°$ (JCPDS 05-0661, 1-0420) [31]. Phase-pure monoclinic CuO crystallites were indicated by major peaks indexed as (1^- 1 1)–(0 0 2) and (1 1 1)–(2 0 0)

planes along with those of elemental Cu (1 1 1), respectively, which agree with the research of Vaseem et al. [27]. The intensities of the diffraction peaks increased with increasing molar concentration of CuO, corresponding to denser CuO NRs. The appearance of peaks characteristic of CuO is indicative of the NRs' high crystallinity.

As can be seen in Fig. 4B, the intensity of reflection gradually increased with increasing molar concentration of CuO, which specifically indicates a higher crystallinity. While smaller, broader peaks were observed in samples prepared at molar concentrations from 10 to 50 mM, sharp, intense peaks were observed for 70, 90 and 110 mM samples. Furthermore, the peaks in Fig. 4B shifted to lower angles by approximately 0.5° when the CuO concentration was changed from 10 mM to 110 mM. In particular, the 2θ values of the $(1^-\ 1\ 1)$–$(0\ 0\ 2)$ and $(1\ 1\ 1)$–$(2\ 0\ 0)$ planes shifted gradually from 36.15° to 35.64° and from 39.32° to 38.95°, respectively, with concurrent increases in peak height due to increasing crystallinity. Also, the peaks at 2θ equal to 32.65°, 68.26°, and 75.18° did not appear in the 10 mM samples but were prominent in the 110 mM samples. All of these data are consistent with increasing crystallinity with increasing concentrations of CuO.

3.3. Dynamic mechanical analyses of hybrid CuO–WCF composite laminates

Fig. 5 shows the storage modulus, *i.e.*, capability to store mechanical energy without dissipation, of hybrid CuO–WCF composite laminates made with various CuO concentrations as a function of temperature. Storage moduli increased with CuO concentration over the entire temperature range. The primary contributors to this enhanced storage modulus are friction and slippage in the presence of high-surface-area CuO NRs. The glass-to-rubber transition temperatures of hybrid CuO–WCF composite laminates were also higher than those of pristine WCF (CuO 0 mM) composite laminates. We believe that the observed enhancements in storage moduli and the increases in glass-to-rubber transition temperatures stem from the reinforcing effects of CuO NRs. In addition, cross-linked interfacial interactions preserved the structural and dimensional stabilities of the composite laminates below 200 °C.

3.4. Piezoresistive response of hybrid CuO–WCF composite laminates

Resistance changes across the interlaminar interface were measured at temperature T, *i.e.*, $\Delta R = R(T) - R_0(T)$, where $R(T)$ and $R_0(T)$ correspond to the resistance values at through-thickness strains ε and 0, respectively [25]. Through-thickness GF was measured *in situ* while Joule heating of the interlaminar interface of hybrid CuO–WCF composite laminates was observed in stage II with an applied current of 2 A and flexural ratio $\varepsilon < 0.8\%$. The interlaminar interface is critical to the mechanical integrity of a structural composite because the piezoresistive response of the composite is attributed to microstructural variations [26]. Fig. 7A and B shows the through-thickness resistance changes across the interlaminar interface at constant cyclic flexural loading during both Joule heating and non-Joule heating.
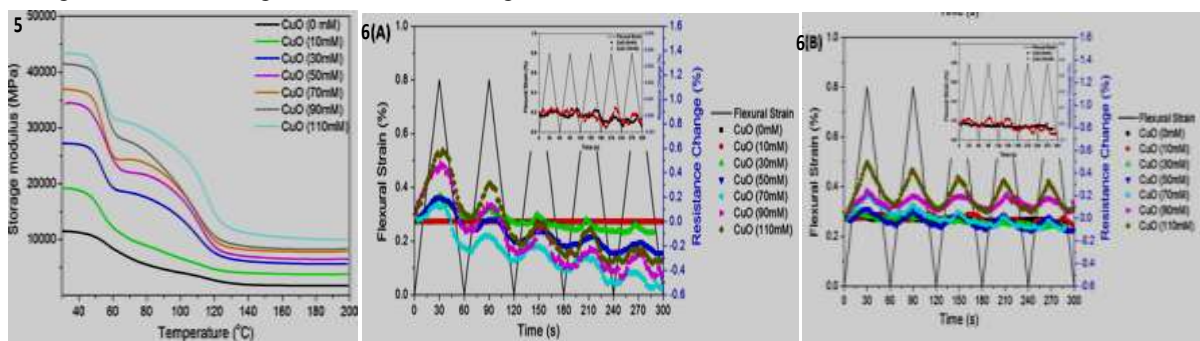
Fig. 5. Temperature-dependent storage modulus of hybrid CuO–WCF composite laminates as a function of CuO molar concentration. **Fig. 6.** Resistance changes across the interlaminar interface in response to *in situ* flexural strain applied to hybrid CuO–WCF composite laminates containing different CuO concentrations (A) during Joule heating and (B) at ambient air temperature.

Furthermore, these resistance changes gradually drifted during 5 min of cyclic flexural loading, as shown in Fig.6A. The drift rate of the resistance change for the prepared composites laminates lowered gradually and the loss of resistance change was irreversible with flexural cycle time [27]. In contrast, resistance changes approached values more typical of piezoresistive phenomena at ambient air temperatures. This was not directly affected by stress-induced microstructural changes, as shown in Fig. 6B. Thus, the interlaminar interface in the thermal resistive heating region contributes to observable resistance changes over time. This effect is due to a greater degree of electron tunneling between laminae via percolative conduction in heating zones, leading to a lower piezoresistive effect and resistance drift as a function of time, compared with the same each composite laminates during non-Joule heating.

The mechanism of the resistance drift is not well understood at present. We believe that strain-induced resistance changes may drift because of capacitance at the interlaminar interface and pressure-induced changes in the band gap at cross-weaved joint junctions between laminae. It is because the band gap is an intimate relation to the conductivity. The correlation between the resistance and band gap in multi-walled carbon nanotube films was exemplified to the report by Cao et al. [25]. The larger number of electron pathways allows for a greater accumulation of current. Therefore, CuO-grafted WCF laminates are excellent candidates for structural energy storage materials. In addition, the high volume concentration of CuO NRs on WCF can act as secondary electron traps, resulting in a pseudo-capacitive effect similar to that observed in a previous report [27].

IV. Conclusions

We report Joule heating and piezoresistive behavior at the interlaminar interface in hybrid CuO–WCF composite laminates. Electrical through-thickness resistance changes were measured as a function of through-thickness strain during three-point bending tests and through-thickness gauge factors were estimated for each material. The resistance of the interface between hybrid CuO–WCF laminae effectively converted electrical energy into thermal energy at relatively larger molar concentrations of CuO up to 110 mM. Heat loss in the absence of applied electric power occurred at a comparatively slower rate due to the presence of CuO NRs in the interlaminar interface, which acted as a thermal barrier composed of resistive heating traps. This phenomenon resulted in a higher resistance to thermal stress regardless of microstructural damage in the elastic regime. Given these properties, electronic excitation during thermal heating of the hybrid CuO–WCF composite laminates results in an accumulation of electric current and resistance drift over time. These materials are potential candidates for structural energy storage applications such as aerodynamic surfaces that require anti-icing coatings or de-icing.

V. Acknowledgements

References

[1] R.F. GibsonA review of recent research on mechanics of multifunctional composite materials and structures, Compos Struct, 92 (12) (2010), pp. 2793-2810

[2] J.W. Sohn, H.S. KimActive recovery of vibration characteristics for delaminated composite structure using piezoelectric actuator, Int J Precis Eng Man, 16 (3) (2015), pp. 597-602

[3] H. Mei, H.Q. Li, Q.L. Bai, Q. Zhang, L.F. ChengIncreasing the strength and toughness of a carbon fiber/silicon carbide composite by heat treatment,Carbon, 54 (2013), pp. 42-47

[4] M.C. Guo, X.S. Yi, G. Liu, L.P. LiuSimultaneously increasing the electrical conductivity and fracture toughness of carbon–fiber composites by using silver nanowires-loaded interleaves,Compos Sci Technol, 97 (2014), pp. 27-33.

[5] Z.L. Jin, X.T. Chen, Y.Q. Wang, D.B. WangThermal conductivity of PTFE composites filled with graphite particles and carbon fibers,Comp Mater Sci, 102 (2015), pp. 45-50

[6] H.W. He, J.L. Wang, K.X. Li, J.A. Wang, J.Y. GuMixed resin and carbon fibres surface treatment for preparation of carbon fibres composites with good interfacial bonding strength, Mater Des, 31 (10) (2010), pp. 4631-4637.

[7] K. Kong, B.K. Deka, J.W. Seo, Y.B. Park, H.W. ParkEffect of CuO nanostructure morphology on the mechanical properties of CuO/woven carbon fiber/vinyl ester composites,Compos A – Appl Sci Manuf, 78 (2015), pp. 48-59.

[8] J.G. Lu, P.C. Chang, Z.Y. FanQuasi-one-dimensional metal oxide materials – synthesis, properties and applications, Mater Sci Eng R, 52 (1–3) (2006), pp. 49-91

[9] P. Poizot, S. Laruelle, S. Grugeon, L. Dupont, J.M. TarasconNano-sized transition-metaloxides as negative-electrode materials for lithium-ion batteries,Nature, 407 (6803) (2000), pp. 496-499

[10] X.P. Gao, J.L. Bao, G.L. Pan, H.Y. Zhu, P.X. Huang, F. Wu, *et al.*Preparation and electrochemical performance of polycrystalline and single crystalline CuO nanorods as anode materials for Li ion battery, J Phys Chem B, 108 (18) (2004), pp. 5547-5551

[11] R.V. Kumar, Y. Diamant, A. GedankenSonochemical synthesis and characterization of nanometer-size transition metal oxides from metal acetates, Chem Mater, 12 (8) (2000), pp. 2301-2305

[12] Dhanasekaran, T. MahalingamSurface modifications and optical variations of (−111) lattice oriented CuO nanofilms for solar energy applications,Mater Res Bull, 48 (9) (2013), pp. 3585-3593.

    a. Fosbury, S.K. Wang, Y.F. Pin, D.D.L. ChungThe interlaminar interface of a carbon fiber polymer–matrix composite as a resistance heating element, Compos A – Appl Sci Manuf, 34 (10) (2003), pp. 933-940.

[13] L.Q. Liu, K.Q. Hong, T.T. Hu, M.X. XuSynthesis of aligned copper oxide nanorod arrays by a seed mediated hydrothermal method, J Alloy Compd, 511 (1) (2012), pp. 195-197.

[14] B.K. Deka, K. Kong, J. Seo, D. Kim, Y.B. Park, H.W. ParkControlled growth of CuO nanowires on woven carbon fibers and effects on the mechanical properties of woven carbon fiber/polyester composites,Compos Part A – Appl Sci Manuf, 69 (2015), pp. 56-63.

[15] C.L. Cao, C.G. Hu, Y.F. Xiong, X.Y. Han, Y. Xi, J. MiaoTemperature dependent piezoresistive effect of multi-walled carbon nanotube films, Diam Relat Mater, 16 (2) (2007), pp. 388-392.

[16] D.J. Wang, D.D.L. ChungThrough-thickness piezoresistivity in a carbon fiber polymer–matrix structural composite for electrical-resistance-based through-thickness strain sensing, Carbon, 60 (2013), pp. 129-138.

[17] S.K. Wang, D.D.L. ChungPiezoresistivity in continuous carbon fiber polymer–matrix composite, Polym Compos, 21 (1) (2000), pp. 13-19.

[18] K. Kong, B.K. Deka, M. Kim, A. Oh, H. Kim, Y.B. Park, *et al.*Interlaminar resistive heating behavior of woven carbon fiber composite laminates modified with ZnO nanorods, Compos Sci Technol, 100 (2014), pp. 83-91.

[19] X.X. Xu, H. Yang, Y.N. LiuSelf-assembled structures of CuO primary crystals synthesized from Cu(CH$_3$COO)(2)-NaOH aqueous systems, CrystEngComm, 14 (16) (2012), pp. 5289-5298.

[20] Y.G. Li, B. Tan, Y.Y. WuAmmonia-evaporation-induced synthetic method for metal (Cu, Zn, Cd, Ni) hydroxide/oxide nanostructures, Chem Mater, 20 (2) (2008), pp. 567-576.

[21] F. Li, K. Tao, B.A. Wentuan, D.C. Li, Z. Li, X.T. HuangVersatile synthesis of rectangular shaped nanobat-like CuO nanostructures by hydrothermal method; structural properties and growth mechanism, Appl Surf Sci, 255 (12) (2009), pp. 6279-6284.

[22] M. Vaseem, A. Umar, S.H. Kim, Y.B. HahnLow-temperature synthesis of flower-shaped CuO nanostructures by solution process: formation mechanism and structural properties, J Phys Chem C, 112 (15) (2008), pp. 5729-5735.

[23] S.K. Wang, D.P. Kowalik, D.D.L. ChungSelf-sensing attained in carbon-fiber–polymer-matrix structural composites by using the interlaminar interface as a sensor, Smart Mater Struct, 13 (3) (2004), pp. 570-592.

[24] Y.G. Jeong, J.E. AnEffects of mixed carbon filler composition on electric heating behavior of thermally-cured epoxy-based composite films, Compos A – Appl Sci Manuf, 56 (2014), pp. 1-7.

[25] F. El-TantawyJoule heating treatments of conductive butyl rubber/ceramic superconductor composites: a new way for improving the stability and reproducibility? Eur Polym J, 37 (3) (2001), pp. 565-574.

[26] C.Z. Shi, X.W. Liu, R.Y. ChuaiPiezoresistive sensitivity, linearity and resistance time drift of polysilicon nanofilms with different deposition temperatures, Sensors-Basel, 9 (2) (2009), pp. 1141-1166.